

# Arbitrary Self-Assembly of Peptide Extracellular Microscopic Matrices\*\*

Angelo Bella, Santanu Ray, Michael Shaw, and Maxim G. Ryadnov\*

Biomimetic extracellular matrices prompt major advances in regenerative medicine.<sup>[1]</sup> Main efforts are being focused on engineering self-assembling peptide fibers. These fibers are nanostructures exhibiting near-crystalline periodicities, which are believed to be necessary for cell–matrix interactions.<sup>[2]</sup> Nanoscale ordering, however, rigidifies the fiber architecture and can hinder the accommodation of subtle morphological alterations inevitable in dynamic cellular environments.<sup>[3]</sup> More adaptive approaches are sought and may include the incorporation of fiber-shaping peptides<sup>[4a,b]</sup> or metal-binding sites,<sup>[4c,d]</sup> biocatalytic<sup>[4e]</sup> induction, or amphiphilic packing.<sup>[4f]</sup> In these designs matrices are furnished by fiber rearrangements or gelation, which, in contrast to the native matrices,<sup>[5a–c]</sup> can restrict branching and porosity to nanometer dimensions.<sup>[4,5d]</sup> The question remains whether a nongelated microscopic scaffold can be designed that would mimic native architectures.<sup>[5a–c]</sup> Herein we describe an arbitrary self-assembly mechanism, which enables the formation of microscopic highly branched peptide matrices. We show that such architectures can be programmed into a single peptide block.

Our approach stems from two interrelated criteria. The assembly 1) must support the formation of intricate fibrillar networks rather than individual fibers and 2) should exhibit positive tropism, being responsive to external stimuli (thermal denaturation) and cell adhesion.

With this in mind we designed a self-assembling peptide, dubbed Cycl\_one (cyclic one), which comprises two domains that oligomerize by forming a parallel coiled-coil heterodimer.<sup>[6]</sup> Each domain pairs with its complementary partner from another copy of the same peptide such that interactions occur between different peptides and not within the same peptide. To ensure this arrangement, the domains were linked through two short linkers and cyclized antiparallel to each other. The linkers provide sufficient spacing only for outward interactions of the antiparallel domains, thus yielding a

bifaceted anisotropic block, which propagates laterally through interfacial interactions of the two domains (Figure 1a,b).

Given that three contiguous heptads provide cooperative and stable coiled coils,<sup>[6d,e]</sup> each domain was made three heptads long. Heptads were designed based on a canonical

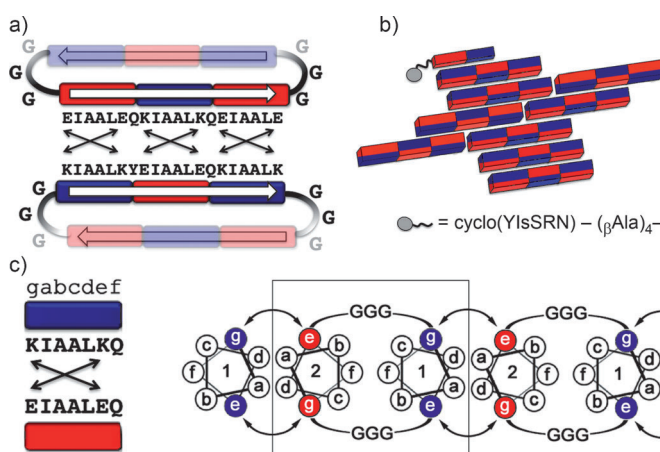


**Figure 1.** Cycl\_one design. a) Bifaceted cyclopeptide block consisting of two domains, which run antiparallel to each other and are separated by two triglycyl linkers. The domains of different copies of the same cyclopeptide block form parallel coiled-coil heterodimers. The block can have four different orientations, two of which are shown. b) Schematic depiction of the arbitrary assembly of the block. The cell adhesion motif (Cam), shown in gray, binds to a cyclopeptide block through a two-heptad coiled-coil stretch. c) Two heptad types; linear sequences and on-coiled-coil helical wheels. One cyclopeptide block is highlighted by the square. Cationic and anionic heptads and residues are in blue and red, respectively; arrows indicate electrostatic interactions between lysine and glutamate residues. G = Gly = glycine, E = Glu = glutamic acid, I = Ile = isoleucine, A = Ala = alanine, L = Leu = leucine, Q = Gln = glutamine, K = Lys = lysine, Y = Tyr = tyrosine, S = Ser = serine, s = D-Ser, R = Arg = arginine, N = Asn = asparagine.

[\*] Dr. S. Ray, M. Shaw, Dr. M. G. Ryadnov

National Physical Laboratory  
Teddington, Middlesex, TW11 0LW (UK)  
E-mail: max.ryadnov@npl.co.uk

Dr. M. G. Ryadnov  
School of Physics and Astronomy, University of Edinburgh  
Edinburgh, EH9 3JZ (UK)

A. Bella  
Department of Chemistry, University of Leicester  
Leicester, LE1 7RH (UK)

[\*\*] We thank the NPL's Strategic research Programme and EPSRC for financial support.



Supporting information for this article is available on the WWW under <http://dx.doi.org/10.1002/anie.201104647>.

repeat pattern of hydrophobic (H) and polar (P) residues, PHPPHPP, usually designated gabcdef (Figure 1c). The combination of isoleucine and leucine residues in positions a and d was chosen to specify the hydrophobic interface of a dimer; small and polar alanine and glutamine residues were used at the solvent-exposed b, c, and f sites to facilitate solubilization of the peptide.<sup>[3a,5d]</sup> A single f site was taken by a tyrosine residue to allow concentration determination by optical absorption measurements. Lysine and glutamate residues occupied g and e sites to provide helix-stabilizing electrostatic g–e' interactions between heptads of different peptides (Figure 1a,c).

The two obtained heptad types, namely anionic heptad EIAALEQ and cationic heptad KIAALKQ, alternate in the domains to enable mixed sequence alignments between different blocks. The block can adopt four different orientations with respect to the plane of the cycle, thereby sustaining multiple modes of assembly. This feature makes the assembly arbitrary. The design rationale is summarized in Figure 1 as well as in Scheme S1 and Table S1 in the Supporting Information.

As probed by circular dichroism (CD) spectroscopy, the domains Ind1 and Ind2 did not fold individually, but gave concentration-dependent helical signals as equimolar mixtures (Ind12; Figure 2 and Figure S1 in the Supporting

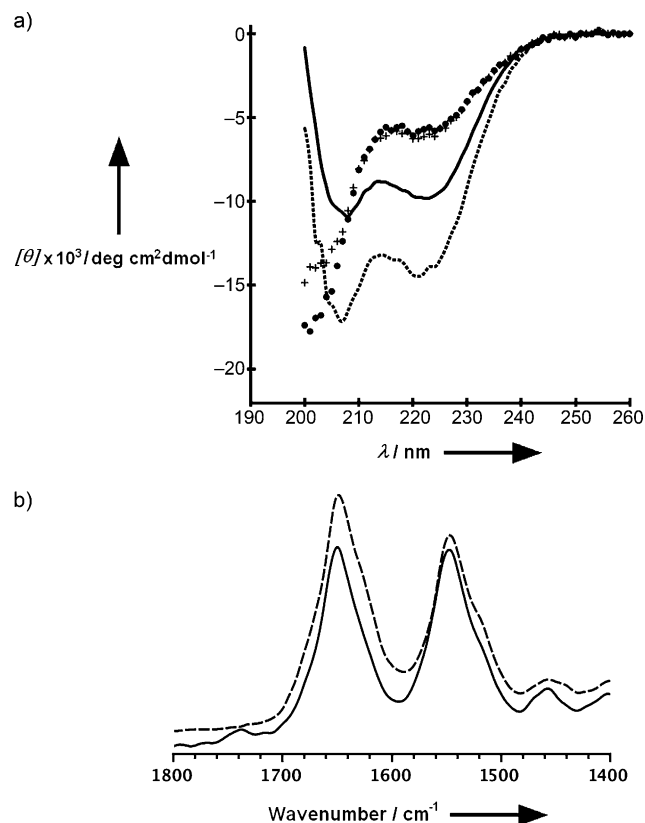


**Figure 2.** Peptide folding. a) CD and b) FTIR spectra for Ind1 (+), Ind2 (●), equimolar mixture of peptides Ind1 and Ind2 (Ind12, dashed lines) and the cyclopeptide Cyclone (solid lines). Samples were at a concentration of 100  $\mu\text{M}$  of each peptide, in 10 mM 3-(*N*-morpholino)-propanesulfonic acid (MOPS), pH 7 at room temperature.

Information). Similarly, increased Cyclone concentrations led to enhanced helicity, the degree of which, however, remained comparatively lower than observed for peptide mixture Ind12 (Figure S1 in the Supporting Information). Thermal unfolding of peptide mixture Ind12 revealed dominating transition midpoints below 40°C with sigmoidal curves, which are characteristic of a cooperatively folded structure (Figure S2 in the Supporting Information). This was not observed for peptide Cyclone, thus suggesting a partial  $\beta$ -sheet transition or structural destabilization upon denaturation (Figure S2 in the Supporting Information).<sup>[4b]</sup> How-

ever, both peptide mixture Ind12 and peptide Cyclone showed complete reversibility of folding (Figures S3 and S4 in the Supporting Information). Furthermore, Fourier transform infrared (FTIR) spectra recorded before and after thermal denaturation were nearly identical for both systems and were dominated by helical bands around 1650 and 1550  $\text{cm}^{-1}$  (Figure 2 and Figures S3 and S4 in the Supporting Information). The half-widths of the bands, which can be used as a measure of the helix stability, were comparable and indicative of moderate helices. This finding was consistent with the CD spectroscopy data. Bands that would point to the formation of intermolecular  $\beta$ -pleated structures (i.e. 1610–1625  $\text{cm}^{-1}$ )<sup>[4b,7]</sup> were not observed.

The spectroscopy results suggest that Cyclone may fold and assemble under formation of reversible helical structures that are deemed sufficiently stable to form high-aspect-ratio microstructures. In accord with this, differential interference contrast, scanning electron, and atomic force microscopy (DIC, SEM, and AFM) showed extensive mesoscopic fibrillar networks that were dominated by multiply branched and interconnected fibrils separated at micrometer distances (Figure 3 and Figure S5 in the Supporting Information). The

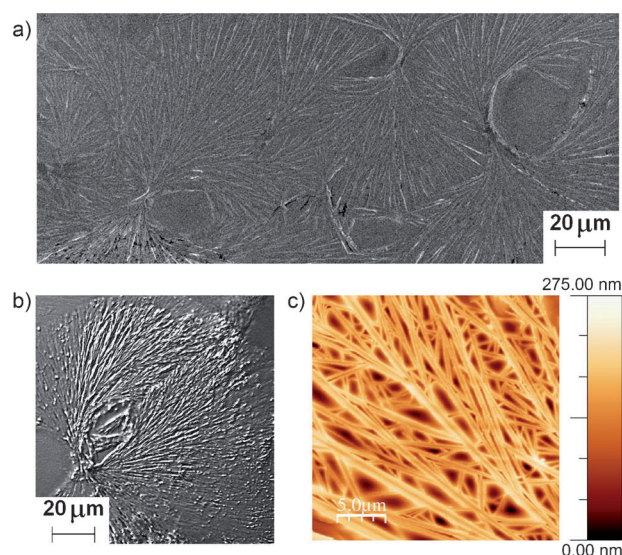


**Figure 3.** Cyclone matrix. a) SEM, b) DIC, and c) AFM images of Cyclone. Samples were at a concentration of 100  $\mu\text{M}$  peptide in 10 mM MOPS, pH 7 at room temperature.

sizes of the observed branches varied from hundreds of nanometers to several micrometers, which was consistent with the size distributions obtained from dynamic light scattering measurements (Figure S6 in the Supporting Information). No assemblies were found for peptide mixture Ind12, thus confirming that the domains did not propagate alone or when matched in the coiled coil (Figure S5 in the Supporting Information). The dimensional parameters of the Cyclone matrix were similar to those of the native collagen and fibrin matrices,<sup>[5]</sup> which points to their potential functional similarities.

Indeed, as gauged by cell proliferation assays, Cycl\_one promoted the proliferation of human dermal fibroblasts with an efficiency nearing 40 % of that of fibrous collagen used as a control (Figure 4). Cell motility was also apparent and similar to that of the collagen substrate (Videos S1 and S2 in the

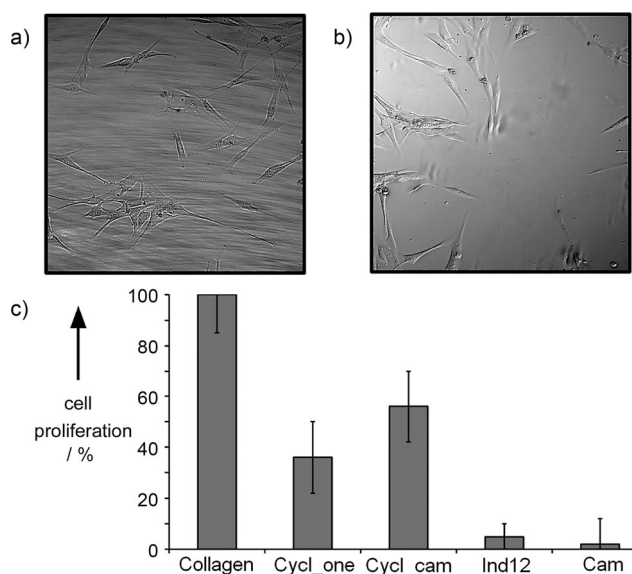


**Figure 4.** Matrix-supported cell proliferation. DIC micrographs for a) human dermal fibroblasts on collagen matrix, b) human dermal fibroblasts on Cycl\_one matrix and c) the comparative proliferation of the fibroblasts on different substrates. Samples were at a concentration of 100  $\mu\text{M}$  total peptide, collagen at 5  $\text{mg mL}^{-1}$ , incubation times 24 h (see also Videos S1 and S2 in the Supporting Information).

Supporting Information). Notably, these assessments were made for Cycl\_one assembled at micromolar concentrations and collagen used at  $\text{mg mL}^{-1}$ . This observation, together with the fact that none of the substrates gelled, suggests that the tensile and surface properties of the Cycl\_one matrix were comparable with those of the collagen. Note that collagen is a natural substrate, which incorporates cell recognition and adhesion motifs.<sup>[5,8]</sup> These motifs were not present in Cycl\_one.

Therefore, to provide a more consistent comparison, the Cycl\_one matrix was decorated with a cell attachment motif (Cam). This is a conformational mimic<sup>[9a]</sup> of the laminin peptide YIGSR<sup>[9b]</sup> conjugated to the N-terminal triskaideka peptide of Ind2 (Scheme S1 in the Supporting Information). The peptide is able to bind to either domain in Cycl\_one and can thereby be incorporated into or onto the matrix (Figure 1 and Table S1 in the Supporting Information).

Mixing the Cam peptide with Cycl\_one matrices at ratios as small as 0.001:1 (Cycl\_cam in Figure 4c) resulted in a 20 % increase of cell proliferation compared with the bare scaffold. This finding implies that the recruitment of the Cam peptide through coiled-coil formation between its tetrakaidecad portion and Cycl\_one domains is competent to provide the necessary exposure of the laminin epitope for cell binding.

In contrast, neither the Cam peptide alone nor peptide mixture Ind12 supported cell proliferation to a significant

extent (Figure 4c). Furthermore, CD and FTIR spectra for the mixture Cycl\_cam revealed that the Cam peptide did not affect helix formation; only a marginal  $\alpha$ - $\beta$  transition was observed after thermal denaturation, thereby suggesting that the Cam peptide is complementary to the assembly (Figure S7 in the Supporting Information). The combined data confirms the defining role of the supramolecular matrix architecture in supporting efficient cell attachment and growth.

In summary, we have described a microscopic architecture of de novo design mimicking that of native extracellular matrices. The matrix is derived from a single peptide block, the arbitrary self-assembly of which leads to the formation of hyperbranched fibrillar networks spanning nano- to micrometer dimensions. The assembly is underlain by reversible helix formation and can accommodate complementary motifs that enhance cell recognition and growth. The designed matrix does not gel and supports cell adhesion, spreading, motility, and proliferation through its local morphology, which resembles that of native fibrillar systems. The introduced assembly mechanism holds promise for engineering cell-supporting supramolecular scaffolds with tailorable functional and structural parameters.

Received: July 5, 2011

Revised: October 12, 2011

Published online: November 23, 2011

**Keywords:** cell adhesion · extracellular matrix · protein design · self-assembly · tissue engineering

- [1] a) J. H. Collier, J. S. Rudra, J. Z. Gasiorowski, J. P. Jung, *Chem. Soc. Rev.* **2010**, 39, 3413–3424; b) M. Zelzer, R. V. Ulijn, *Chem. Soc. Rev.* **2010**, 39, 3351–3357; c) H. Cui, M. J. Webber, S. I. Stupp, *Biopolymers* **2010**, 94, 1–18.
- [2] a) G. A. Silva, C. Czeisler, K. L. Niece, E. Beniash, D. A. Harrington, J. A. Kessler, S. I. Stupp, *Science* **2004**, 303, 1352–1355; b) V. Jayawarna, M. Ali, T. A. Jowitt, A. F. Miller, A. Saiani, J. E. Gough, R. V. Ulijn, *Adv. Mater.* **2006**, 18, 611–614; c) E. F. Banwell, E. S. Abelardo, D. J. Adams, M. A. Birchall, A. Corrigan, A. M. Donald, M. Kirkland, L. C. Serpell, M. F. Butler, D. N. Woolfson, *Nat. Mater.* **2009**, 8, 596–600; d) R. G. Ellis-Behnke, Y. X. Liang, S. W. You, D. K. Tay, S. Zhang, K. F. So, G. E. Schneider, *Proc. Natl. Acad. Sci. USA* **2006**, 103, 5054–5059; e) R. N. Shah, N. A. Shah, M. M. Del Rosario Lim, C. Hsieh, G. Nuber, S. I. Stupp, *Proc. Natl. Acad. Sci. USA* **2010**, 107, 3293–3298.
- [3] a) D. Papapostolou, A. M. Smith, E. D. Atkins, S. J. Oliver, M. G. Ryadnov, L. C. Serpell, D. N. Woolfson, *Proc. Natl. Acad. Sci. USA* **2007**, 104, 10853–10858; b) L. E. O’Leary, J. A. Fallas, J. D. Hartgerink, *J. Am. Chem. Soc.* **2011**, 133, 5432–5443; c) S. Rele, Y. Song, R. P. Apkarian, Z. Qu, V. P. Conticello, E. L. Chaikof, *J. Am. Chem. Soc.* **2007**, 129, 14780–14787; d) E. T. Pashuck, H. Cui, S. I. Stupp, *J. Am. Chem. Soc.* **2010**, 132, 6041–6046; e) F. W. Kotch, R. T. Raines, *Proc. Natl. Acad. Sci. USA* **2006**, 103, 3028–3033.
- [4] a) M. G. Ryadnov, D. N. Woolfson, *Nat. Mater.* **2003**, 2, 329–332; b) M. G. Ryadnov, D. N. Woolfson, *J. Am. Chem. Soc.* **2005**, 127, 12407–12415; c) C. M. Micklitsch, P. J. Knerr, M. C. Branco, P. Nagarkar, D. J. Pochan, J. P. Schneider, *Angew. Chem.* **2011**, 123, 1615–1617; *Angew. Chem. Int. Ed.* **2011**, 50, 1577–1579; d) S. N. Dublin, V. P. Conticello, *J. Am. Chem. Soc.* **2008**, 130, 49–51; e) A. R. Hirst, S. Roy, M. Arora, A. K. Das, N. Hodson, P. Murray,

- S. Marshall, N. Javid, J. Sefcik, J. Boekhoven, J. H. van Esch, S. Santabarbara, N. T. Hunt, R. V. Ulijn, *Nat. Chem.* **2011**, *2*, 1089–1094; f) H. Dong, S. E. Paramonov, J. D. Hartgerink, *J. Am. Chem. Soc.* **2008**, *130*, 13691–13695.
- [5] a) A. E. Brown, R. I. Litvinov, D. E. Discher, P. K. Purohit, J. W. Weisel, *Science* **2009**, *325*, 741–744; b) T. Starborg, Y. Lu, A. Huffman, D. F. Holmes, K. E. Kadler, *Scand. J. Med. Sci. Sports* **2009**, *19*, 547–552; c) N. Huebsch, D. J. Mooney, *Nature* **2009**, *462*, 426–432; d) M. G. Ryadnov, A. Bella, S. Timson, D. N. Woolfson, *J. Am. Chem. Soc.* **2009**, *131*, 13240–13241.
- [6] a) B. Apostolovic, M. Danial, H.-A. Klok, *Chem. Soc. Rev.* **2010**, *39*, 3541–3575; b) M. G. Ryadnov, *Biochem. Soc. Trans.* **2007**, *35*, 487–491; c) D. N. Woolfson, *Adv. Protein Chem.* **2005**, *70*, 79–112; d) J. E. Rozzelle, A. Tropsha, B. W. Erickson, *Protein Sci.* **2008**, *3*, 345–355; e) J. Su, R. S. Hodges, C. M. Kay, *Biochemistry* **1994**, *33*, 15501–15510.
- [7] a) N. A. Nevskaya, Y. N. Chirgadze, *Biopolymers* **1976**, *15*, 637–648; b) W. K. Surewicz, H. H. Mantsch, D. Chapman, *Biochemistry* **1993**, *32*, 389–394.
- [8] a) P. Castillo-Briceño, D. Bihan, M. Nilges, S. Hamaia, J. Meseguer, A. Garcia-Ayala, R. W. Farndale, V. Mulero, *Mol. Immunol.* **2011**, *48*, 826–834; b) J. Heino, *Bioessays* **2007**, *29*, 1001–1010.
- [9] a) A. Bella, H. Lewis, J. Phu, A. R. Bottrill, S. C. Mistry, C. E. Pullar, M. G. Ryadnov, *J. Med. Chem.* **2009**, *52*, 7966–7969; b) J. Graf, Y. Iwamoto, M. Sasaki, G. R. Martin, H. K. Kleinman, F. A. Robey, Y. Yamada, *Cell* **1987**, *48*, 989–996.